MINERALOGIA POLONICA
Vol. 14, No 1—2 — 1983

Elżbieta BODEK, Janusz ZIĘTKIEWICZ*, Mieczysław ŻYŁA**

SORPTION PROPERTIES AND POROSITY OF SOME CATIONIC FORMS OF MONTMORILLONITE AND THEIR ACID-ACTIVATION PRODUCTS

UKD 549.623:552.52] montmorillonit. 01:541.183.5:546.293+539.217.1

Abstract. The paper discusses the changes in sorption properties and porosity of Na–, Zn–, Al–, Cr– and Sn– forms of montmorillonite and their acid-activation products. A substantial increase in pore volume has been noted, especially in the range of micro- and mesopores. Most pronoucned changes occur in sodium montmorillonite. The change in porosity is peralleled by the marked increase in argon sorption on acid-activated samples. In acid-activation products, a considerable decrease in sorption can be observed, due to the removal of OH^- groups and exchangeable cations from the interlayer spaces of montmorillonite.

INTRODUCTION

The sorption properties of clay minerals depend on the chemical nature of their surface, i.e. on the concentration of sorption polar centres at the surfaces accessible to adsorbates. The chemical nature of surface affects the sorption properties of these minerals with respect to vapours of both polar and nonpolar substances. In this case, the essential factors are the electrostatic interaction between the adsorbate molecules and the montmorillonite surface centres and the hydration of exchangeable cations. Another important factor is the geometry of the system montmorillonite — kinetic diameter of adsorbate molecules. In the case of adsorption of small molecules of chemical compounds, the well developed microporous structure is of prime importance. When larger molecules are adsorbed, the system of mesopores plays a significant role in the process.

The changes in the sorption properties of montmorillonite during acid modification of its porous structure were noticed by Crepaz et al. (1966), Nowak and Gregor (1969) and Fijał et al. (1975). These authors studied the changes in specific surface areas determined from argon, water and methyl alcohol sorption, occurring in the process of acid activation of montmorillonite in response to the change in the chemical character of its surface. It was also found that the time of acid activation of montmorillonite had an effect on its oil-decolourizing ability. Studying the effect of acid activation time (at acid boiling point), Nowak and Gregor (1969) noticed

* Institute of Chemical Conversion of Coal and Physicochemistry of Sorbents, Academy of Mining and Metallurgy in Cracow (Kraków, al. Mickiewicza 30).

that the greatest increase in surface area took place in initial periods of time. This increase was accounted for by partial degradation of the octahedral sheet caused by the removal of Mg^{2+} and Fe^{2+} ions. The present authors (Fijał et al. 1975) carried out investigations of sorption of polar (water, methyl alcohol) and nonpolar (argon, n-hexane) substances on the products of acid activation as a function of time and noticed that there were two maxima of sorption properties with respect to argon and n-hexane, corresponding to 3- and 10-hour activation. These changes were attributed to the change in morphology of acid activation products. Nowak (1973) studied changes in the morphology of acid-activated montmorillonite and found that at the initial stage of activation the volume of pores of a radius of 4.8—6 Å increased and did not change up to 24 hours of activation. He also noticed similar changes for pores of a radius of 6—15 Å. The volume of pores of a radius greater than 30 Å increased progressively during 5-hour activation and then decreased again. It was also found that the degree of changes in specific surface areas versus activation time depended on the provenance of montmorillonite.

EXPERIMENTAL

The aim of this paper was to determine the effect of interlayer cations on the sorption properties and porosity of some cationic forms of montmorillonite and their corresponding acid-activation products.

Activation was carried out with 20% hydrochloric acid solution at 373 K for 4 hours. Montmorillonite was separated by sedimentation from bentonite of the Chmielnik deposit and converted into sodium form with 1 n NaCl solution. Then Zn^{2+}, Al^{3+}, Cr^{3+} and Sn^{2+} cations were substituted for sodium cations, using respective 1 n chloride solutions. The ratio of sediment to solution was assumed to be 1:20.

Isotherms for water vapour adsorption were obtained at 293 K using microrburettes for liquids (Lasoń, Żyła 1963). Argon adsorption isotherms were determined at 77.5 K with sorption manostats (Ciembroniewicz, Lasoń 1972). Pore measurements were made with a Carlo-Erba porosimeter.

RESULTS

Adsorption studies

Adsorption and porosimetric studies were carried out on sodium, zinc, aluminium and chromium forms of montmorillonite and the corresponding acid-activation products. Figures 1, 2, 3 and 4 present isotherms obtained for water vapour and argon sorption and desorption on sodium and zinc montmorillonites and the corresponding acid-activated forms.

Using the BET equation, a_m values and specific surface areas S were calculated for all samples from the parts of isotherms corresponding to pressures $p/p_0 = 0.05$—-0.35. These parameters were treated as indices of sorption changes, and the respective values for untreated montmorillonite samples are given in Table 1.

Specific surface areas determined from water vapour sorption are several times greater than argon surface areas, which is due to specific sorption of water vapour

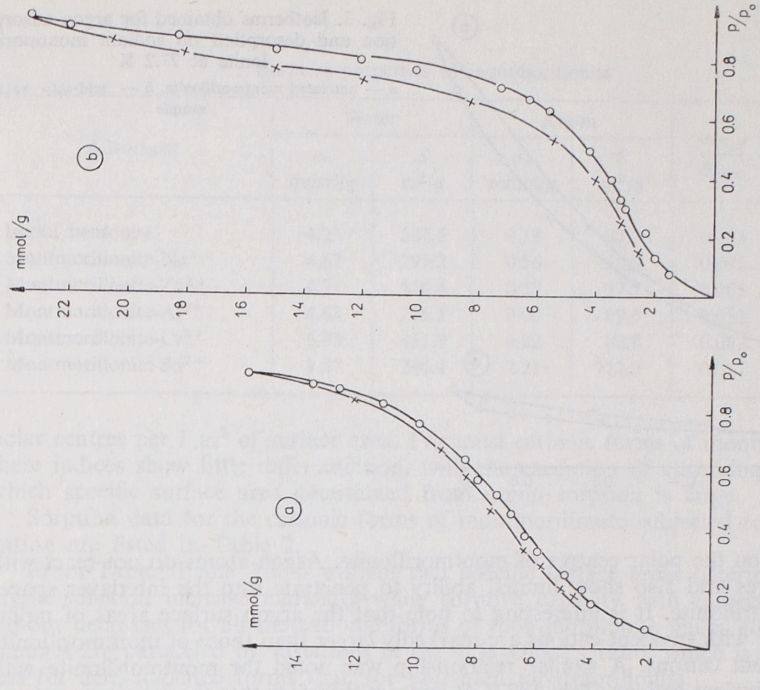

Fig. 2. Isotherms obtained for water vapour adsorption and desorption on zinc montmorillonite at 298.2 K
a — untreated montmorillonite, *b* — acid-activated sample

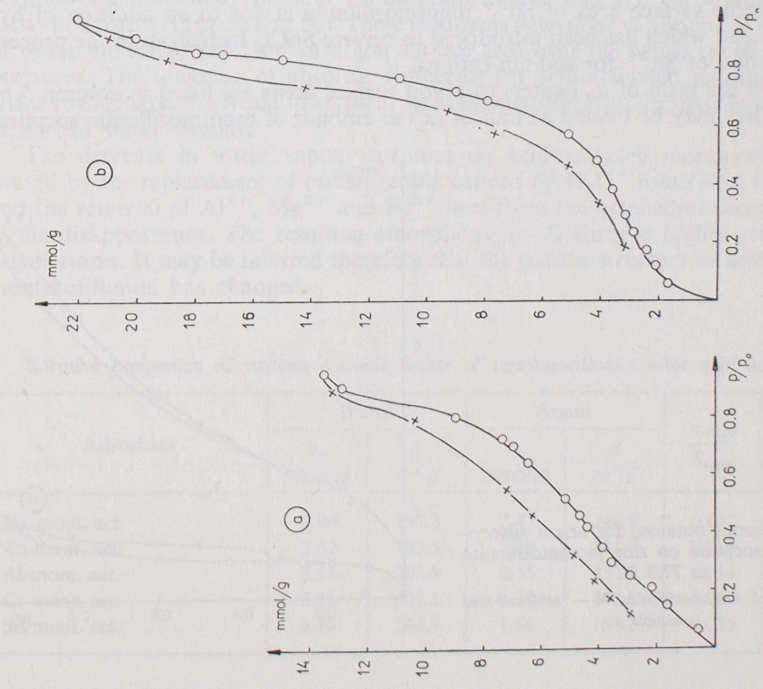

Fig. 1. Isotherms obtained for water vapour adsorption and desorption on sodium montmorillonite at 298.2 K
a — untreated montmorillonite, *b* — acid-activated sample

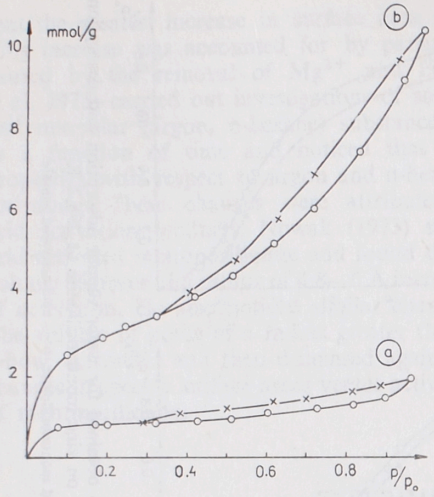

Fig. 3. Isotherms obtained for argon adsorption and desorption on sodium montmorillonite at 77.2 K

a — untreated montmorillonite, *b* — acid-activated sample

molecules on the polar centres of montmorillonite. Argon atoms do not react with these centres and also show limited ability to penetrate into the interlayer spaces of montmorillonite. It is interesting to note that the argon surface areas of montmorillonite with trivalent cations are markedly larger than those of montmorillonite with bivalent cations. A similar relationship was noted for montmorillonite with uni- and bivalent cations (Żyła 1972). It appears therefore that the interlayer cations have a significant effect on the morphology of montmorillonite. The high value for the specific surface area of Sn^{2+} montmorillonite is due to an addition of hydrochloric acid which has been introduced to reverse $SnCl_2$ hydrolysis in the process of substitution of Sn^{2+} for sodium cations.

Data on the ratio of a_m (water) to argon surface areas are listed in column 5 of Table 1. They may be treated as indices of the amount of montmorillonite sorption

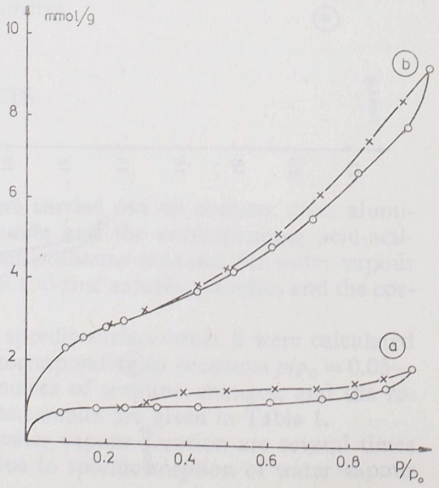

Fig. 4. Isotherms obtained for argon adsorption and desorption on zinc montmorillonite at 77.2 K

a — untreated montmorillonite, *b* — acid-activated sample

Table 1

Sorptive properties of montmorillonite

Adsorbent	Water		Argon		$\frac{a_{mH_2O}}{S_{argon}}$	$\frac{S_{H_2O}}{S_{argon}}$
	a_m mmol/g	S m²/g	a_m mmol/g	S m²/g		
Initial bentonite	4.23	267.5	0.38	37.3	0.113	7.14
Montmorillonite-Na^+	4.67	295.2	0.56	56.9	0.082	5.02
Montmorillonite-Zn^{2+}	4.91	310.4	0.57	57.7	0.085	5.38
Montmorillonite-Al^{3+}	4.68	295.5	0.89	89.5	0.052	3.30
Montmorillonite-Cr^{3+}	6.83	431.8	0.82	82.9	0.082	5.21
Montmorillonite-Sn^{2+}	3.87	244.4	2.21	222.7	0.017	1.09

polar centres per 1 m² of surface area. For most cationic forms of montmorillonite these indices show little differentiation, with the exception of chromium form for which specific surface area determined from argon sorption is large.

Sorption data for the cationic forms of montmorillonite subjected to acid activation are listed in Table 2.

From Tables 1 and 2 it is evident that specific surface areas determined from argon sorption increase markedly while sorptive capacity with respect to water vapour decreases for all the cationic forms of montmorillonite under study. These changes are paralleled by variations in the $a_m H_2O/S_{argon}$ ratio, which is 3—7 times less for acid-activated forms than for untreated montmorillonite.

Worth noting is the shape of absolute isotherms obtained for water vapour sorption on untreated Na- and Zn-montmorillonite and the corresponding acid-activated forms (Figs. 5a and 5b). These isotherms determine variations in the amount of water molecules per 1 m² of argon surface area over the whole range of relative pressures. The lowering of absolute isotherms for acid-activated montmorillonites is due to the marked increase in argon areas at the simultaneous decrease in the amount of sorbed water vapour.

The decrease in water vapour sorption on acid-activated montmorillonites is caused by the replacement of exchangeable cations by H_3O^+ ions (Fijał et al. 1976) and the removal of Al^{3+}, Mg^{2+} and Fe^{2+} ions from the octahedral sheet, attended by its disappearance. The resulting amorphous Si—O form is highly accessible to argon atoms. It may be inferred therefore that the porous structure of acid-activated montmorillonite has changed.

Table 2

Sorptive properties of various cationic forms of montmorillonite after acid activation

Adsorbent	Water		Argon		$\frac{a_{mH_2O}}{S_{argon}}$	$\frac{S_{H_2O}}{S_{argon}}$
	a_m mmol/g	S m²/g	a_m mmol/g	S m²/g		
Na-mont. act.	3.04	192.3	2.47	249.9	0.012	0.77
Zn-mont. act.	2.57	162.5	2.29	231.9	0.011	0.70
Al-mont. act.	3.24	205.0	2.35	237.9	0.014	0.86
Cr-mont. act.	6.35	401.1	4.38	442.8	0.014	0.90
Sn-mont. act.	4.19	264.9	1.66	168.2	0.025	1.57

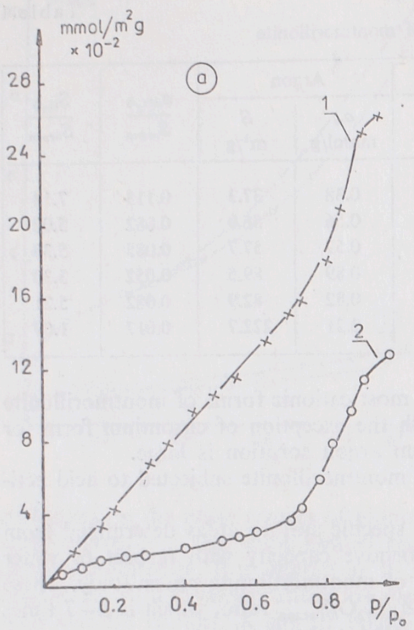

Fig. 5a. Absolute isotherms for water determined on sodium montmorillonite

1 — untreated montmorillonite, *2* — acid-activated sample

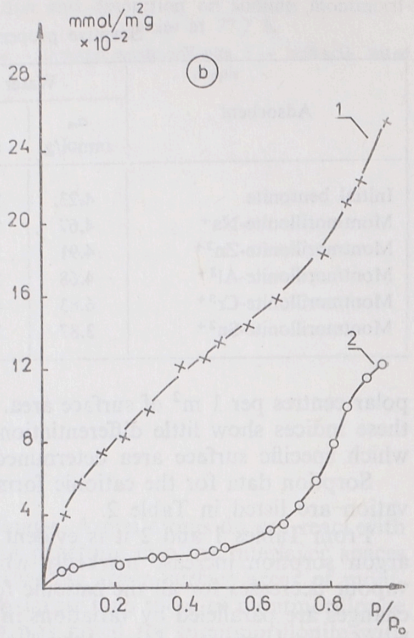

Fig. 5b. Absolute isotherms for water determined on zinc montmorillonite

1 — untreated montmorillonite, *2* — acid-activated sample

To determine the microporosity of montmorillonite in the process of acid activation, adsorption measurements were made in the range of very low argon vapour pressures. The isotherms obtained were used to estimate the total volume of micropores. The following equation of Dubinin's theory developed on the basis of potential adsorption theory of Polany was used:

$$\lg a = \lg a_o - D(\lg p_o/p)^2$$

where: a — amount of adsorbed vapour (mmol/g),
D — constant characterizing the adsorbent-adsorbate system at given temperature.

From the boundary value a_o determined graphically from sorption data W_o, i.e. the volume of liquid adsorbate required to fill the micropore volume of 1 g of adsorbent, was calculated. The W_o values expressed in cm^3 of liquid argon, determined for the montmorillonite samples studied and their corresponding acid-activation products, are given in Table 3. As appears from the Table, acid activation results in a 2.5-fold increase in W_o, corresponding to the 2.5-fold increase in micropore volume. Particularly wide differences have been noted for chromium montmorillonite and the respective acid-activated form.

Table 3

Micropores volume W_o ($cm^3/g \cdot 10^{-2}$) for various cationic forms of montmorillonite

Sample	Cationic form				
	Na^+	Zn^{2+}	Al^{3+}	Cr^{3+}	Sn^{2+}
non-activated	1.082	1.192	1.919	1.773	5.117
activated	4.710	3.838	4.361	8.257	4.594

The changes in pore size of activated montmorillonites have been confirmed by the pore volume distribution determined as a function of pore radius. According to the capillary condensation theory (Żółcińska-Jezierska 1974), the adsorbate condenses in capillaries at pressures lower than saturated vapour pressure, the more readily the smaller the capillary radius. To calculate the capillary radius Kelvin's equation is used, relating the radius of concave spherical liquid meniscus with vapour pressure at equilibrium state

$$r_K = \frac{2V\sigma}{RT \ln p_o/p}$$

where: r_K — Kelvin capillary radius,
σ — surface tension of liquid adsorbate,
V — molar volume of liquid adsorbate.

Basing on the above equation, the distribution of pore volume vs. capillary radius was calculated from the desorption part of the argon sorption isotherm (Zdanov) (Figs. 6, 7). The dominant pores in the structure of montmorillonite are mesopores of radii ranging from 1.6 to 2.5 nm. Of untreated montmorillonite samples Al— and

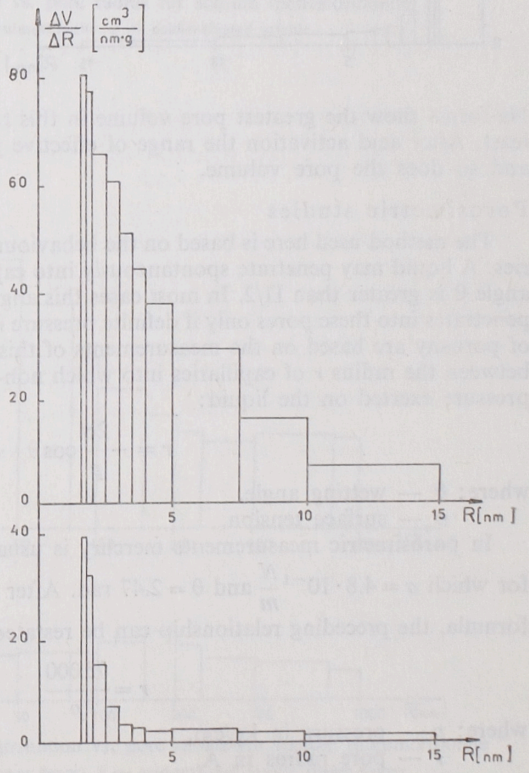

Fig. 6. Pore volume distribution vs. effective radius for sodium montmorillonite

a — untreated montmorillonite (lower figure), *b* — acid-activated sample (upper figure)

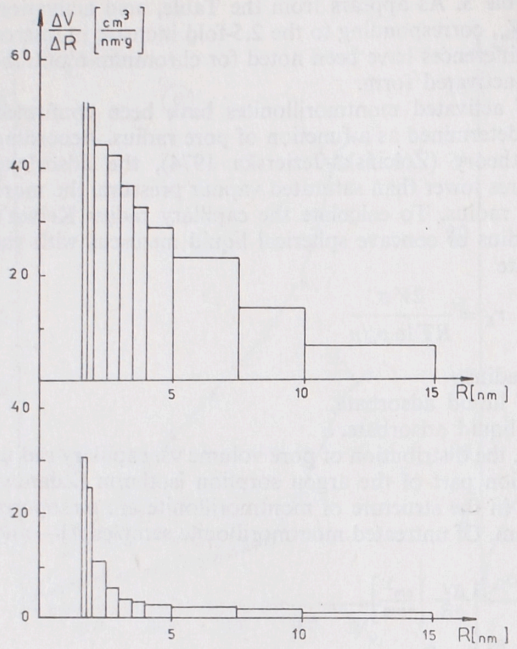

Fig. 7. Pore volume distribution vs. effective radius for zinc montmorillonite

a — untreated montmorillonite (lower figure), *b* — acid-activated sample (upper figure)

Na-forms show the greatest pore volume in this range and Zn-montmorillonite the least. After acid activation the range of effective pore radius increases up to 2 nm and so does the pore volume.

Porosimetric studies

The method used here is based on the behaviour of non-wetting liquids in capillaries. A liquid may penetrate spontaneously into capillaries provided that the wetting angle θ is greater than Π/2. In most cases this angle is less than Π/2, and the liquid penetrates into these pores only if definite pressure is exerted. The proper calculations of porosity are based on the measurements of this pressure. There is a relationship between the radius *r* of capillaries into which non-wetting liquid penetrates and the pressure exerted on the liquid:

$$r = -\frac{2\sigma}{p}\cos\theta$$

where: θ — wetting angle,
σ — surface tension.

In porosimetric measurements mercury is usually used as a non-wetting liquid, for which $\sigma = 4.8 \cdot 10^{-1}\frac{N}{m}$ and $\theta = 2.47$ rad. After substituting these values into the formula, the preceding relationship can be restated in the form:

$$r = \frac{75000}{p}$$

where: *p* — pressure in kg/cm,
r — pore radius in Å.

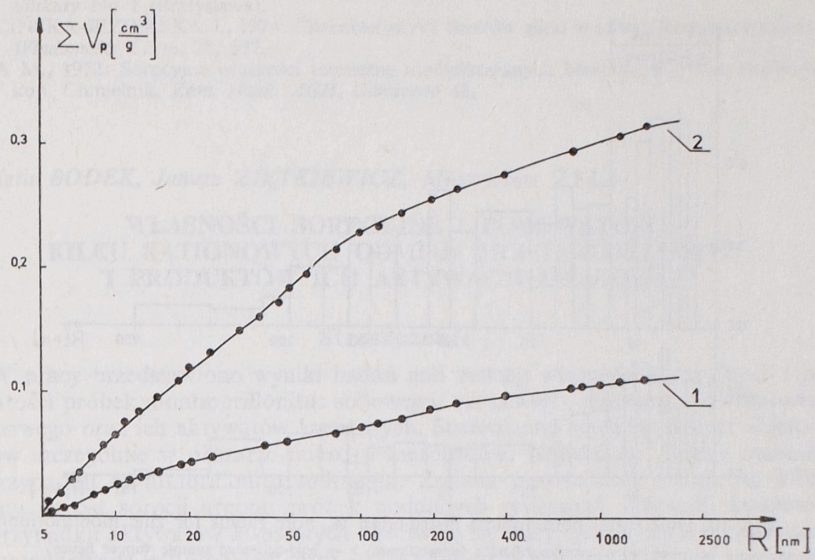

Fig. 8. Total pore volume vs. pore radius for sodium montmorillonite

1 — untreated montmorillonite, *2* — acid-activated sample

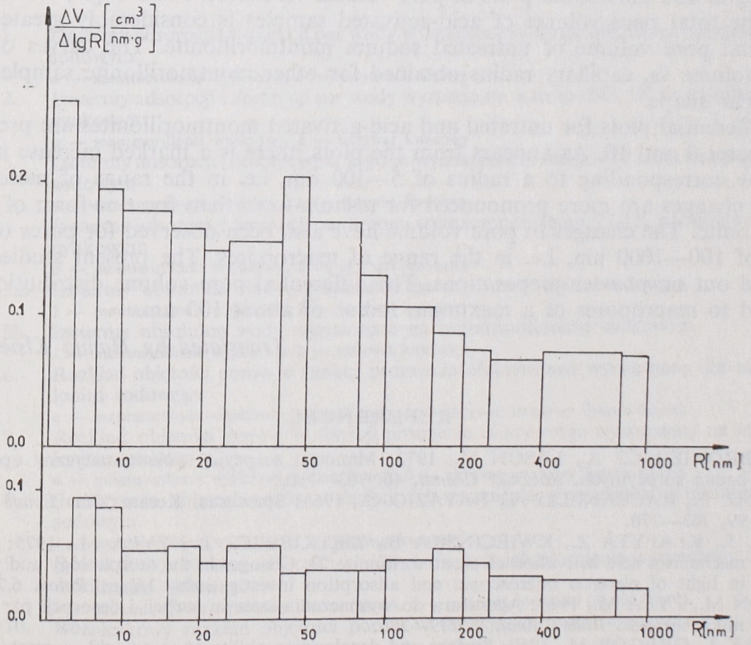

Fig. 9. Differential pore volume distribution vs. pore radius for sodium montmorillonite

a — untreated montmorillonite (lower figure), *b* — acid-activated sample (upper figure)

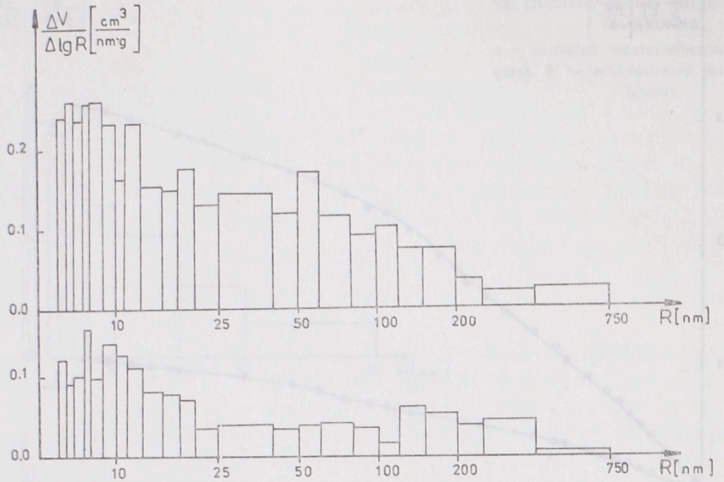

Fig. 10. Differential pore volume distribution vs. pore radius for zinc montmorillonite
a — untreated montmorillonite (lower figure) *b* — acid-activated sample (upper figure)

The porosimeter used in the present studies permits one to follow the changes in pore volume over the range of 5—7500 nm. The results are presented in the form of integral and differential plots of pore volume vs. radius. From Fig. 8 it is evident that the total pore volume of acid-activated samples is considerably greater than the total pore volume of untreated sodium montmorillonite. The curves of total pore volume vs. capillary radius obtained for other montmorillonite samples have a similar shape.

Differential plots for untrated and acid-activated montmorillonites are presented in Figures 9 and 10. As appears from the plots, there is a marked increase in pore volume corresponding to a radius of 5—100 nm, i.e. in the range of mesopores. These changes are more pronounced for sodium-form than for zinc-form of montmorillonite. The changes in pore volume have also been observed for pores of a radius of 100—1000 nm, i.e. in the range of macropores. The present studies were carried out on powder preparations. The differential pore volume distribution was limited to macropores of a maximum radius of about 100 nm.

Translated by Hanna Kisielewska

REFERENCES

CIEMBRONIEWICZ A., LASOŃ M., 1972: Manostat sorpcyjny półautomatyczny aparat do badań sorpcyjnych. *Roczniki Chemii*, 46, 703—710.

CREPAZ E., RACCANELLI A., NAVAZIO G., 1966: Sprechsaal Keram. *Glas Email Silikate* 99, 763—770.

FIJAŁ J., KŁAPYTA Z., KWIECIŃSKA B., ZIĘTKIEWICZ J. i ŻYŁA M., 1975: On the mechanism acid activation of montmorillonite. II. Changes in the morphology and porosity in light of electron microscopic and adsorption investigations, *Miner. Polon.* 6.2.

LASOŃ M., ŻYŁA M., 1963: Aparatura do wyznaczania izoterm sorpcji i desorpcji par metodą mikrobiuretek. *Chem. Anal.* 8, 279—286.

NOVAK J., GREGOR M., 1969: Surface and decolorizing ability of some acid — treated montmorillonites. Reprinted from the proceedings of the international clay conference. Vol. 1, 851—857 Tokyo.

NOVAK J., 1973: Changes in montmorillonite morphology in the course of acid destruction. *Silikaty* No 1 (Bratysława).

ŻÓŁCIŃSKA-JEZIERSKA J., 1974: Charakterystyka tlenków glinu w świetle badań sorpcyjnych. *Wiadomości Chem.* 28, 857.

ŻYŁA M., 1972: Sorpcyjne własności termiczne modyfikowanych bentonitów i montmorillonitu kop. Chmielnik. *Zesz. Nauk. AGH, Górnictwo* 48.

Elżbieta BODEK, Janusz ZIĘTKIEWICZ, Mieczysław ŻYŁA

WŁASNOŚCI SORPCYJNE I POROWATOŚĆ KILKU KATIONOWYCH ODMIAN MONTMORILLONITU I PRODUKTÓW ICH AKTYWACJI KWASOWEJ

Streszczenie

W pracy przedstawiono wyniki badań nad zmianą własności sorpcyjnych i porowatości próbek montmorillonitu: sodowego, cynkowego, glinowego, chromowego i cynawego oraz ich aktywatów kwasowych. Stwierdzono wyraźny wzrost objętości porów szczególnie w obszarze mikro- i mezoporów. Największe zmiany zachodzą w przypadku montmorillonitu sodowego. Zmiana porowatości rzutuje na kilkakrotny wzrost sorpcji argonu próbek poddanych procesowi aktywacji kwasowej. W przypadku aktywatów kwasowych obserwuje się duży spadek sorpcji cząsteczek, co spowodowane jest ubytkiem grup —OH i kationów międzypakietowej przestrzeni montmorillonitu.

OBJAŚNIENIA FIGUR

Fig. 1. Izotermy adsorpcji i desorpcji par wody wyznaczone w temp. 298,2 K na montmorillonicie sodowym
a — montmorillonit wyjściowy, *b* — aktywat kwasowy

Fig. 2. Izotermy adsorpcji i desorpcji par wody wyznaczone w temp. 298, 2K na montmorillonicie cynkowym
a — montmorillonit wyjściowy, *b* — aktywat kwasowy

Fig. 3. Izotermy adsorpcji i desorpcji par argonu wyznaczone w temp. 77,2 K na montmorillonicie sodowym
a — montmorillonit wyjściowy, *b* — aktywat kwasowy

Fig. 4. Izotermy adsorpcji i desorpcji par argonu wyznaczone w temp. 77,2 K na montmorillonicie cynkowym
a — montmorillonit wyjściowy, *b* — aktywat kwasowy

Fig. 5a. Izotermy absolutne wody wyznaczone na montmorillonicie sodowym
1 — montmorillonit wyjściowy, 2 — aktywat kwasowy

Fig. 5b. Izotermy absolutne wody wyznaczone na montmorillonicie cynkowym
1 — montmorillonit wyjściowy, 2 — aktywat kwasowy

Fig. 6. Rozkład objętości porów w funkcji promienia efektywnego wyznaczony dla montmorillonitu sodowego
a — montmorillonit wyjściowy (dolna figura), *b* — aktywat kwasowy (górna figura)

Fig. 7. Rozkład objętości porów w funkcji promienia efektywnego wyznaczony na montmorillonicie cynkowym
a — montmorillonit wyjściowy, (dolna figura), *b* — aktywat kwasowy (górna figura)

Fig. 8. Sumaryczna objętość porów w funkcji ich promienia wyznaczona na montmorillonicie sodowym
1 — montmorillonit wyjściowy *2* — aktywat kwasowy

Fig. 9. Różniczkowy rozkład objętości porów w funkcji ich promienia wyznaczony dla montmorillonitu sodowego
a — montmorillonit wyjściowy (dolna figura), *b* — aktywat kwasowy (górna figura)

Fig. 10. Różniczkowy rozkład objętości porów w funkcji ich promienia wyznaczony na montmorillonicie cynkowym
a — próbka wyjściowa (dolna figura), *b* — aktywat kwasowy (górna figura)

Эльжбета БОДЭК, Януш ЗЕНТКЕВИЧ, Мечислав ЖИЛА

СОРБЦИОННЫЕ СВОЙСТВА И ПОРИСТОСТЬ НЕСКОЛЬКИХ КАТИОННЫХ РАЗНОВИДНОСТЕЙ МОНТМОРИЛЛОНИТА И ПРОДУКТОВ ИХ КИСЛОТНОЙ АКТИВАЦИИ

Резюме

В работе представлены результаты исследований изменений сорбционных свойств и пористости образцов натриевого, цинкового, алюминиевого, хромового и оловянного монтмориллонитов, а также их кислотных активатов. Констатировано явный рост объема пор, в частности в области мезо- и микропор. Наибольшие изменения имеют место в случае натриевого монтмориллонита. Изменение пористости вызывает несколькократный рост сорбции аргона образцов, подверженных процессу кислотной активации. В случае кислотных активатов наблюдается большое уменьшение сорбции частиц, что вызвано убытком групп —ОН и катионов межпакетного пространства монтмориллонита.

ОБЪЯСНЕНИЯ К ФИГУРАМ

Фиг. 1. Изотермы адсорбции и десорбции паров воды, определенные в температуре 298,2 К на натриевом монтмориллоните
a — исходный монтмориллонит, *b* — кислотный активат

Фиг. 2. Изотермы адсорбции и десорбции паров воды, определенные в температуре 298,2 К на цинковом монтмориллоните
a — исходный монтмориллонит, *b* — кислотный активат

Фиг. 3. Изотермы адсорбции и десорбции паров аргона, определенные в температуре 77,2 К на натриевом монтмориллоните
a — исходный монтмориллонит, *b* — кислотный активат

Фиг. 4. Изотермы адсорбции и десорбции паров аргона, определенные в температуре 77,2 К на цинковом монтмориллоните
a — исходный монтмориллонит, *b* — кислотный активат

Фиг. 5a. Абсолютные изотермы воды, определенные на натриевом монтмориллоните
1 — исходный монтмориллонит, *2* — кислотный активат

Фиг. 5b. Абсолютные изотермы воды, определенные на цинковом монтмориллоните
1 — исходный монтмориллонит, *2* — кислотный активат

Фиг. 6. Распределение объема пор в функции эффективного радиуса, определенное для натриевого монтмориллонита
a — исходный монтмориллонит (нижняя фигура), *b* — кислотный активат (верхняя фигура)

Фиг. 7. Распределение объема пор в функции эффективного радиуса, определенное на цинковом монтмориллоните
a — исходный монтмориллонит (нижняя фигура), *b* — кислотный активат (верхняя фигура)

Фиг. 8. Суммарный объем пор в функции их радиуса, определенный на натриевом монтмориллоните
1 — исходный монтмориллонит, *2* — кислотный активат

Фиг. 9. Дифференциальное распределение объема пор в функции их радиуса, определенное для натриевого монтмориллонита
a — исходный монтмориллонит (нижняя фигура), *b* — кислотный активат (верхняя фигура)

Фиг. 10. Дифференциальное распределение объема пор в функции их радиуса, определенное на цинковом монтмориллоните
a — исходный монтмориллонит (нижняя фигура), *b* — кислотный активат (верхняя фигура)